DAS Over Multimode Fibers With Reduced Fading by Coherent Averaging of Spatial Modes

Daniele Orsuti, Gianluca Marcon, Axel Turolla, Marco Santagiustina, Andrea Galtarossa, Massimo Zampato, and Luca Palmieri

***Abstract*— We investigate the performance of distributed acoustic sensing over multi-mode fibers based on heterodyne phase-sensitive optical time-domain reflectometry. We report a mathematical model describing the relation between phase variation and applied strain in the presence of multi-mode propagation that supports the feasibility of distributed acoustic measurements over multi-mode fibers. We also propose a novel coherent averaging method that achieves up to a three-fold reduction of the noise floor compared to state-of-the-art methods.**

***Index Terms*— Phase sensitive OTDR, multimode fibers, spatial-division multiplexing, coherent averaging.**

I. Introduction

RAYLEIGH-BASED fiber-optic distributed acoustic sensors (DAS) have attracted increasing attention in recent years due to their unique features [1]. While most DAS systems use single-mode fibers (SMFs), there is a growing interest in extending DAS to multi-mode fibers (MMFs). One of the main driving interests is to leverage the existing MMF infrastructure in the oil and gas industries, which is currently used for Raman-based temperature monitoring [2]. A few works started investigating DAS over MMFs, however, primarily focusing on few-mode fibers and not analyzing how the proposed method would scale to MMFs [3], [4], [5]. Regardless of whether the optical fiber is single- or multi-mode, phase-sensitive optical time domain reflectometry (ϕ-OTDR) is one of the most commonly used DAS configurations [1]. In recent years, a lot of effort has been put to deal with the signal fading issue of ϕ-OTDR systems, which is due to both intra-pulse coherent interference and polarization variation along the fiber. Recent techniques have tackled the coherent fading issue combining independent measurements channels (e.g., extracted from different frequency bands) carrying the same disturbance information, which are coherently averaged using techniques such as the so called rotated-vector-sum (RVS) [6], [7]. When DAS is applied to MMFs, mode coupling is an additional issue that needs to be faced; nevertheless, the spatial modes can be used also to reduce signal fading, since they act as independent measurement channels.

In this letter, expanding a preliminary analysis [8], we experimentally and theoretically analyze the feasibility of DAS measurements over MMFs. The proposed setup relies on a three-mode photonic lantern (PhL) as a mode de/multiplexer to exploit the spatial diversity to improve the measurement reliability [9], [10]. Moreover, we also propose a novel coherent averaging method that is optimal in terms of mean-squared error (MSE) and outperforms the RVS method.

Manuscript received 27 April 2023; accepted 6 June 2023. Date of publication 13 June 2023; date of current version 23 June 2023. This work was supported in part by EniProgetti SpA; and in part by the Italian Ministry for Education, University and Research (MIUR), Departments of Excellence, under Grant 232/2016. *(Corresponding author: Daniele Orsuti.)*

Daniele Orsuti, Gianluca Marcon, Marco Santagiustina, Andrea Galtarossa, and Luca Palmieri are with the Department of Information Engineering, University of Padova, 35131 Padua, Italy (e-mail: daniele.orsuti@phd.unipd.it).

Axel Turolla and Massimo Zampato are with EniProgetti SpA, 30175 Venezia, Italy.

Color versions of one or more figures in this letter are available at https://doi.org/10.1109/LPT.2023.3285625.

Digital Object Identifier 10.1109/LPT.2023.3285625

II. Theoretical Model

Fundamentally, DAS in SMFs is made possible by the fact that the phase of the propagating light varies linearly with the strain applied to the fiber. This holds true also for MMFs, but only for each mode individually; differently, the relation between the phase of the total light field and the applied strain may be nonlinear in general. The phase variations measured by a DAS reflect what happens in the perturbed fiber sections, whose length, L, is typically shorter than the DAS gauge length and hence in the order of meters. In a MMF, the electric field transmitted across one of these sections can be written as $\boldsymbol{E}_{\text{out}} = \sum_m a_m \exp\{-j(2\pi/\lambda)n_m L\}\boldsymbol{E}_m$, where the sum extends over the propagating modes, n_m is the effective index of mode m, $\boldsymbol{E}_m$ its field distribution (we omitted the transverse coordinates for brevity), and a_m its complex amplitude. The perturbed fiber sections are typically no longer than a few meters and in such a short distance the action of the strain is not strong enough to induce a significant transfer of power from one mode to another. In a SMF scenario, this power transfer would correspond to a polarization change, which is indeed largely and safely ignored in DAS systems. For these reasons, the coefficients a_m can be assumed constant.

Consistently with the typical assumption made for SMF-based DAS, we assume that the strain is constant over the perturbed fiber section. Therefore, the phase term of $\boldsymbol{E}_{\text{out}}$ varies from $(2\pi/\lambda)n_m L$ to $(2\pi/\lambda)n_m L + \Delta\phi_m$, with

$$\Delta\phi_m = \frac{2\pi}{\lambda} n_0 L \left[\left(1 + \frac{\Delta n_m}{n_0} + \frac{\delta n_m}{n_0} \right) \epsilon + \frac{\delta n_m}{n_0} \right], \quad (1)$$

where ϵ is the applied axial strain, which induces the elongation $L \rightarrow L(1+\epsilon)$ and the refractive index change $n_m \rightarrow (n_m + \delta n_m)$; moreover, we set $n_m = n_0 + \Delta n_m$, with n_0 denoting the effective index of the fundamental mode (used here as a reference) and Δn_m is the modal birefringence between the fundamental mode and the mode m [11]. For each mode, the refractive index change is related to the applied strain by the relation $\delta n_m \approx -0.1\, n_m^3 \epsilon$ [1]; therefore, δn_m can

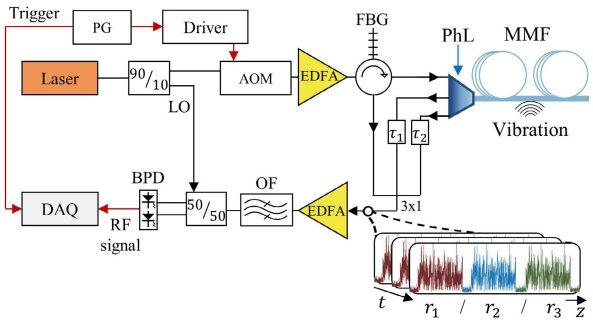

Fig. 1. Experimental Setup. PG: Pulse generator; $\tau_n (n = 1, 2)$: fiber delay line; $r_m (m = 1, 2, 3)$: spatial mode de-multiplexed by the PhL; FBG: fiber Bragg grating filter; OF: Optical filter; RF: radio-frequency.

be approximated to the first order in the modal birefringence as $\delta n_m \approx -0.1\ n_0^3 \epsilon (1 + 3\Delta n_m / n_0)$. Inserting this expression into (1), and considering only terms up to the first order in ϵ, we find $\Delta\phi_m \approx \frac{2\pi}{\lambda} n_0 (1 - 0.1\ n_0^2) L\epsilon + \frac{2\pi}{\lambda} \Delta n_m (1 - 0.3 n_0^2) L\epsilon$, where the first term is the usual strain-induced phase shift observed in SMFs [1], whereas the second term is an extra phase shift characteristic of each higher-order mode. It is then clear that the relation between the phase of the transmitted field $\boldsymbol{E}_{\text{out}}$ and the applied strain is linear only as long as this extra phase shift is much smaller than both the first term (but this is always verified since $\Delta n_m \ll n_0$) and 2π. Due to the round-trip, the phase shift measured by the DAS is actually twice the one calculated before. Therefore, the above condition yields

$$\epsilon \ll \frac{\lambda}{2\left(1 - 0.3 n_0^2\right) \Delta n_m L}. \tag{2}$$

This theoretical result sets an upper bound to the strain applied to the fiber, above which DAS in MMFs would lose linearity. This bound is inversely proportional to the perturbed fiber section. Moreover, it is also inversely proportional to the modal birefringence, which means that MMFs with less modal dispersion, such as graded-index ones, enable measurements on a wider strain range. Considering as an example $L = 2$ m, $n_0 \approx 1.47$, and assuming $\max\{\Delta n_m\} \approx 10^{-3}$, (2) yields $\epsilon \ll 1.1$ mϵ, which is quite a loose constraint considering the typical strain values of the perturbations encountered in DAS measurements [12].

III. Methods

A. Experimental Setup

To validate the feasibility of performing DAS measurements over MMFs, we implemented the heterodyne ϕ-OTDR scheme shown in Fig. 1. The output of a narrow-linewidth laser is split by a 90:10 coupler into two branches. One branch acts as the local-oscillator (LO); the other branch is modulated by an acousto-optic modulator (AOM) into rectangular pulses of 100 ns duration with a 110 MHz frequency shift. The pulses are launched into a 3-km-long OM2 MMF fiber (50/125 μm) through one of the ports of a three-mode PhL (Phoenix Photonics 3-PL), which acts also as a spatial demultiplexer for the Rayleigh backscattered light. The PhL is realized by a few mode fiber supporting the LP_{01}, LP_{11a}, and LP_{11b} modes; the connection between the PhL and the OM2 fiber is realized through a splice, which is adiabatically tapered to minimize its insertion losses and maximize its return losses. In principle, the three spatial modes demultiplexed by the PhL should be sent to three different receivers. For simplicity, in this experiment the three modes have been multiplexed in time by means of fiber delay lines, so to use a single receiver; this comes at the expense of a three-fold reduction of the achievable acoustic bandwidth. The lengths of the fiber delay lines are about 7 km and 14 km, respectively, so that the introduced delays avoid the overlap of the backscattered traces from the 3-km-long MMF link demultiplexed by the PhL. The probe pulse repetition rate is consequently set to $T_{\text{rep}} = 110\ \mu$s. The beating between the LO and the backscattered light is detected by a balanced-photodiode (BPD) with a 400 MHz bandwidth and digitized at 500 MS/s by a 12-bit data acquisition (DAQ) board. The in-phase (I) and quadrature (Q) components of the backscattered field are obtained with conventional digital I/Q demodulation.

B. LMS Coherent Averaging

The information obtained from independent measurements of the same event needs to be optimally combined, or averaged, into a single result. Let $r_m(t_n, z_k)$ denote the complex value of the Rayleigh backscattered trace of the spatial mode m, at an arbitrary position z_k, and at time t_n. We call a "sequence" the set of values that $r_m(t_n, z_k)$ takes for specific mode and position over N_T consecutive time samples. Sequences from two different modes but at the same position are affected by the same acoustic perturbation; nonetheless, they have an arbitrary, unpredictable and mode-dependent phase offset, θ_m, that prevent their direct averaging. Therefore, before the average can be performed, the phases of the sequences must be aligned. The RVS method achieves this alignment by selecting a reference time instant t_1, and determining the phase offsets of each spatial mode as $\theta_m = \arg\{r_m(t_1)\}$ [6]. Nevertheless, no indication is given for the selection of this reference time, and, indeed, a poor choice compromises the phase alignment and subsequent averaging. To deal with this issue, the recently proposed double-averaging RVS (DA-RVS) method uses N_T consecutive time samples of a randomly preselected sequence, and use them to compute a refined time-domain-averaged estimate of the phase offsets [13]. The method proposed in this letter proceeds in two steps. First, the sequence with the highest energy over the N_T time samples is selected as the reference sequence. Then, the phase offsets are computed solving a least-mean-square (LMS) problem that yields the optimum phase offsets values that align each other sequence to the reference one. We refer to the proposed method as the LMS method. In details, assume that $\bar{r}(t_n) = \text{argmax}_m \sum_{n=1}^{N_T} |r_m(t_n)|^2$ is the reference sequence according to the highest-energy criterion; we determine the phase offset needed to align the generic sequence $r_m(t_n)$ to $\bar{r}(t_n)$ by seeking the angle θ_m that minimizes the cost function $\mathcal{E} = \sum_n w(t_n) |\bar{r}(t_n) - r_m(t_n) \exp(j\theta_m)|^2$, where $n = 1, \ldots, N_T$, and $w(t_n) = |\bar{r}(t_n)||r_m(t_n)|$ is used to enhance the weight of the higher amplitude samples. Solving the relative LMS problem yields the optimal estimate of the phase θ_m as $\theta_m = \arg\left\{\sum_{n=1}^{N_T} w(t_n) \bar{r}^*(t_n) r_m(t_n)\right\}$. We remark that this choice is optimal in the MSE sense. After estimating the phase offsets, θ_m, with either the RVS, DA-RVS, or the LMS methods, we compute the coherent average as follows: $r(t_n) = (1/M) \sum_m r_m(t_n) \exp(j\theta_m)$.

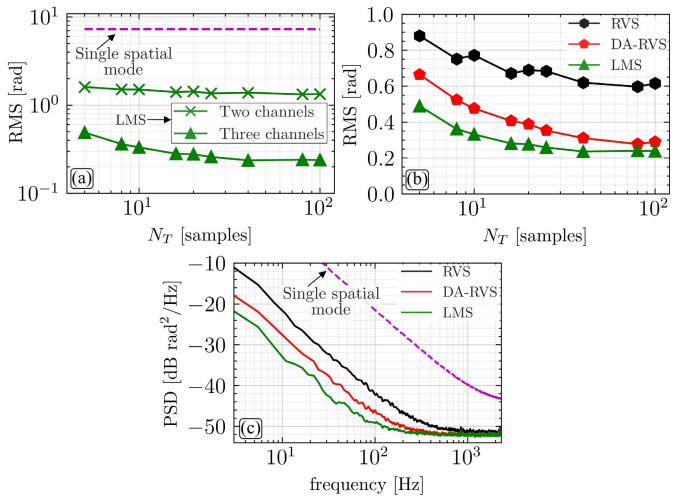

Fig. 2. RMS value of local phase variation versus the temporal window size N_T over which the phase offsets are computed for (a) an increasing number of spatial modes averaged with the LMS method: the single spatial mode curve is the average performance over all 3 modes, whereas the two spatial modes curve is the average performance over all the 3 possible combinations of two modes; (b) three spatial modes averaged with different methods. (c) PSD averaged over all fiber locations for the curves in (b) at $N_T = 25$ samples.

IV. Experimental Results

A. Spatial Modes Averaging

To determine the advantages of using spatial diversity and the performance of the LMS method, we evaluated the root mean square (RMS) value of the local phase variation without mechanical perturbations applied to the MMF. In these settings, any deviation from zero can be attributed to noise. The gauge length to compute the local phase variation is set to 10 m. The RMS value is evaluated over all fiber locations considering 1.1 s of data acquired by the DAQ, which correspond to 1.1 s/T_{rep} = 10,000 time samples. To investigate the impact of the temporal window size N_T on the quality of the estimated phase offsets, the 10,000 time samples were segmented into chunks of N_T time samples, with N_T in the range $5 \div 100$ samples. For each chunk, the RVS, DA-RVS, and LMS methods estimate the phase offsets, which are then used to compute the coherent average chunk-wise. Consecutive chunks overlap by 1 time sample, so as to retain the continuity of the phase signal.

Figure 2(a) shows the RMS value, estimated over the whole fiber length, of the local phase variation versus the time window size N_T. The dashed line refers to the single spatial mode performance, which is independent of N_T; whereas, the cross markers and the triangular markers refer to the LMS average of two and three spatial modes, respectively. As expected, the RMS decreases as the number of averaged modes increases, with a significant drop compared to considering each spatial mode separately. The RMS achieved by the LMS method also decreases as N_T increases because the detection of the reference sequence with the highest energy becomes more accurate for higher N_T values. Figure 2(b) compares the LMS method with the RVS and DA-RVS methods when all three spatial modes are averaged. LMS outperforms the other methods, due to the more accurate selection of the reference sequence and the MSE-optimal estimate of the phase offsets. The RMS reduction saturates as N_T increases; therefore, in the following investigations we set $N_T = 25$ samples. Figure 2(c) shows the power spectral density (PSD) averaged over all fiber locations. At low frequency values, the LMS method achieves lower PSD values than the other methods; this is explained by the lower amount of residual fading points achieved by LMS after the averaging operation.

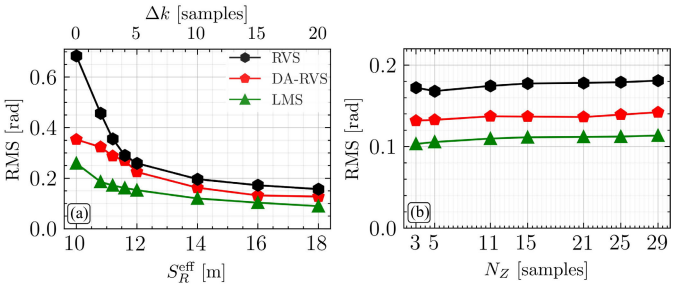

Fig. 3. RMS of the phase noise floor when exploiting both spatial and longitudinal diversity, for $N_T = 25$. (a) $N_Z = 3$ and Δk varies; (b) $\Delta k = 15$ and N_Z varies.

B. Longitudinal Averaging

So far we analyzed how to reduce signal fading by exploiting the spatial mode diversity. In what follows, we generalize this method by exploiting the information diversity carried by the z-samples of the measured Rayleigh backscattered trace. It is not uncommon that φ-OTDR systems oversample the backscattered trace, so that the spacing between consecutive z-samples is typically much smaller than the gauge length [12]. Therefore, including a few sampling points in the analysis rather than just one, causes a marginal degradation of the spatial resolution, while giving the opportunity to exploit also a longitudinal diversity. Actually, a number N_Z of sampling points close to each other, can be treated as N_Z independent measurements of the same event, to which coherent averaging can be applied to further reduce fading. The performance of this average depends on the spectral content of the probe pulse. In general, the closer to Fourier-limited the probe pulse, the more correlated are the z-samples, and hence less information can be obtained by exploiting longitudinal diversity. In this perspective, the best performance is expected with non-Fourier-limited probe pulses [12]. To some extent, this approach is analogous to the frequency-diversity one proposed in [7]; however, the present one is more general, since it does not require any assumptions on the pulse spectral shape. Previous works reported alternative methods for leveraging longitudinal diversity, yet relying on specific fiber configurations, such as wrapping the fiber around a cylindrical cavity structure [14], or restricting the processing to seismic DAS data [15]. In the experimental setting of Fig. 1, we use pulses of 100 ns, which yield a spatial resolution S_R of about 10 m, and we sample the backscattered traces at 500 MS/s, which corresponds to a sampling step δz of about 20 cm. Moreover, the bandwidth of the digital band-pass filter employed for I/Q demodulation is set to 30 MHz, so as to retain the first two side lobes of the sinc-shaped backscattered field spectrum. This parameter setting suggests that even samples closer than S_R could be sufficiently uncorrelated to make longitudinal diversity effective. To test this claim, for each spatial mode and for each sample at arbitrary position z_k, we consider also the samples at $z_k \pm \Delta k \cdot \delta z$. This gives a

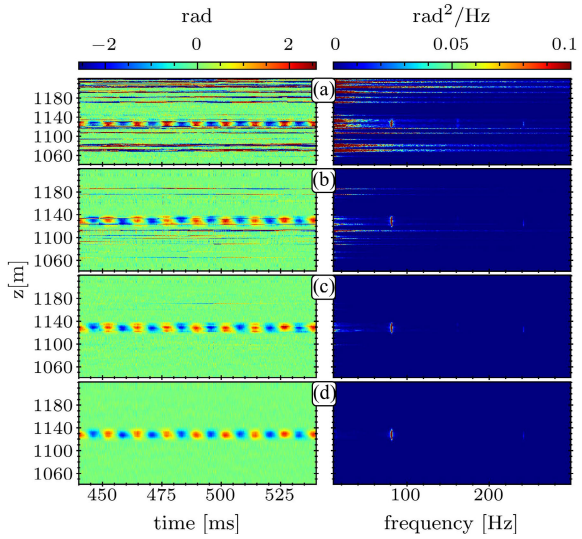

Fig. 4. Spatio-temporal maps (left column) and spectrograms (right column) in presence of a 80 Hz sinusoidal vibration. (a) single spatial mode; LMS average of (b) two spatial modes, (c) three spatial modes, and (d) three spatial modes with longitudinal diversity using $N_Z = 3$ and $\Delta k = 15$.

total of $M \cdot N_Z = 9$ sequences ($M = 3$ modes and $N_Z = 3$ longitudinal samples) over which to compute the coherent average with the above described methods. The parameter Δk controls the distance between the averaged samples; the larger Δk, the lower their statistical correlation, yet the worst the effective spatial resolution $S_R^{\text{eff}} = S_R + 2\Delta k \cdot \delta z$. The results are shown in Fig. 3(a), where the RMS of the phase noise floor is plotted versus Δk (top x-axis) and S_R^{eff} (bottom x-axis) for each of the three averaging method considered so far; $\Delta k = 0$ corresponds to the case when no longitudinal diversity is considered. Clearly, all methods benefit from longitudinal-diversity averaging for increasing distance between samples, until the RMS almost saturates for $\Delta k \approx 15$. Note that this value corresponds to a distance of about 3 m, consistently with the 30 MHz bandwidth of the I/Q band-pass filter. Basically, beyond this distance samples are almost completely uncorrelated and the RMS reduction achieved by the averaging is maximum. We may also test if, for a fixed maximum distance Δk, there is any benefit in considering more than 3 samples in the range $z_k \pm \Delta k \cdot \delta z$. The answer is no, as shown in Fig. 3(b) where the RMS for $\Delta k = 15$ is plotted as a function of N_Z: the RMS shows negligible variation as a function of N_Z, meaning that the samples within the range are too much statistically correlated to provide any advantage in the averaging. To investigate the response of the system to dynamic strain, we inserted a fiber shaker at about 1.1 km from the input. The spatio-temporal maps of the local phase variation in presence of a 80-Hz sinusoidal perturbation and the corresponding spectrograms (computed over the whole acquisition time of 1.1 s) are shown in the left and right columns of Fig. 4, respectively. Figure 4(a) shows the results for a single spatial mode; it can be seen that the local phase variation is strongly compromised by interference fading and polarization fading. Figures 4(b) and 4(c) show the results of the LMS average of two spatial modes and three spatial modes, respectively; when all the three spatial modes are averaged, fading errors are significantly reduced. On the spectrogram maps, it can be observed the presence of a faint third-order harmonic at about 240 Hz, which is attributed to the non-ideal response of the fiber shaker. Figure 4(d) shows the results for the coherent average carried out jointly across the three spatial modes and across the z-axis with parameters $N_Z = 3$ and $\Delta k = 15$; remarkably, the phase variation faithfully reconstructs the applied perturbation without fading errors.

V. Conclusion

In this letter we investigated DAS over MMFs, which is useful in scenarios like oil and gas plants where MMFs are already installed for temperature monitoring. We reported a mathematical model supporting the feasibility of DAS over MMF. Moreover, we proposed a novel coherent averaging method to reduce fading in backscattered traces; we also extended the method to longitudinal diversity, trading spatial resolution for phase accuracy. The proposed coherent averaging method can reduce the noise floor by up to three times compared to state-of-the-art methods.

References

[1] L. Palmieri, L. Schenato, M. Santagiustina, and A. Galtarossa, "Rayleigh-based distributed optical fiber sensing," *Sensors*, vol. 22, no. 18, p. 6811, Sep. 2022.

[2] I. Ashry et al., "A review of distributed fiber-optic sensing in the oil and gas industry," *J. Lightw. Technol.*, vol. 40, no. 5, pp. 1407–1431, Mar. 2022.

[3] M. Chen, A. Masoudi, F. Parmigiani, and G. Brambilla, "Distributed acoustic sensor based on a two-mode fiber," *Opt. Exp.*, vol. 26, no. 19, Sep. 2018, Art. no. 25399.

[4] Z. Zhao et al., "Interference fading suppression in φ-OTDR using space-division multiplexed probes," *Opt. Exp.*, vol. 29, no. 10, p. 15452, May 2021.

[5] B. Lu et al., "Ultra-low-noise MIMO distributed acoustic sensor using few-mode optical fibers," *J. Lightw. Technol.*, vol. 40, no. 9, pp. 3062–3071, May 1, 2022.

[6] D. Chen, Q. Liu, and Z. He, "Phase-detection distributed fiber-optic vibration sensor without fading-noise based on time-gated digital OFDR," *Opt. Exp.*, vol. 25, no. 7, p. 8315, Apr. 2017.

[7] Y. Wu, Z. Wang, J. Xiong, J. Jiang, S. Lin, and Y. Chen, "Interference fading elimination with single rectangular pulse in Φ-OTDR," *J. Lightw. Technol.*, vol. 37, no. 13, pp. 3381–3387, Jul. 1, 2019.

[8] D. Orsuti et al., "Coherent combination method applied to distributed acoustic sensing over deployed multicore fiber," *Proc. 27th Opt. Fiber Sensors Conf.*, 2022, Art. no. 1264323.

[9] A. Galtarossa, L. Palmieri, and M. Zampato, "Optical fiber vibration measurement system in multiphase flows with related method to monitor multiphase flows," U.S. Patent 2 016 103 200, Jun. 25, 2019.

[10] A. Galtarossa, L. Palmieri, and M. Zampato, "Reflectometric vibration measurement system and relative method for monitoring multiphase flows," U.S. Patent WO 2 016 103 201, Apr. 28, 2020.

[11] L. Palmieri and A. Galtarossa, "Coupling effects among degenerate modes in multimode optical fibers," *IEEE Photon. J.*, vol. 6, no. 6, pp. 1–8, Dec. 2014.

[12] J. Pastor-Graells, H. F. Martins, A. Garcia-Ruiz, S. Martin-Lopez, and M. Gonzalez-Herraez, "Single-shot distributed temperature and strain tracking using direct detection phase-sensitive OTDR with chirped pulses," *Opt. Exp.*, vol. 24, no. 12, Jun. 2016, Art. no. 13121.

[13] Y. Wakisaka, D. Iida, H. Oshida, and N. Honda, "Fading suppression of φ-OTDR with the new signal processing methodology of complex vectors across time and frequency domains," *J. Lightw. Technol.*, vol. 39, no. 13, pp. 4279–4293, Jul. 2021.

[14] Z. Wang et al., "Practical performance enhancement of DAS by using dense multichannel signal integration," *J. Lightw. Technol.*, vol. 39, no. 19, pp. 6348–6354, Oct. 2021.

[15] J. B. Ajo-Franklin et al., "Distributed acoustic sensing using dark fiber for near-surface characterization and broadband seismic event detection," *Sci. Rep.*, vol. 9, no. 1, p. 1328, Feb. 2019.

Open Access funding provided by 'Università degli Studi di Padova' within the CRUI CARE Agreement